CPC(HEP & NP), 2010, **34**(2): 182–185 Chinese Physics C Vol. 34, No. 2, Feb., 2010

Unified fission model for proton emission*

DONG Jian-Min(董建敏)[1] ZHANG Hong-Fei(张鸿飞)[1;1)] ZUO Wei(左维)[1,2] LI Jun-Qing(李君清)[2]

[1] School of Nuclear Science and Technology, Lanzhou University, Lanzhou 730000, China
[2] Institute of Modern Physics, Chinese Academy of Sciences, Lanzhou 730000, China

Abstract The unified fission model (UFM) combining with the phenomenological assault frequency has been carried out to investigate the proton-radioactivity half-lives of spherical proton emitters. The results are in good agreement with the experimental data and other theoretical values, and newly observed spherical proton emitters have been analyzed. Finally, the effect of angular momentum transfer on half-life of proton emission has been discussed in detail and a formula can be used to describe this relationship.

Key words proton emission, half-life, unified fission model

PACS 23.50.+z, 21.10.Tg

1 Introduction

The study of exotic nuclei has became a very interesting topic both from the experimental and theoretical points of view with the development of the radioactive beam facilities and led to the discovery of a new form of radioactivity-proton emission. The nuclei around the proton drip line represent one of the fundamental limits of nuclear existence and these with such a large excess of protons undergo spontaneous proton emission towards stability. In addition, the rapid proton capture process which plays a very important role in nuclear astrophysics has its inverse in the proton radioactivity from the nuclear ground state or low isomeric states. Therefore the study of the proton emission is significant. The first example of proton emission from nuclei was observed in an isomeric state of ^{53}Co in 1970. With the improvement in experimental facilities, examples of proton radioactivity from ground states or low lying isomeric states have been identified between $Z=51$ and $Z=83$ [1]. The proton radioactivity can be used as an useful tool to extract some nuclear structure information such as the shell structure and the coupling between bound and unbound nuclear states [2]. In addition to this experimental development, we were also motivated to investigate proton emission theoretically. As α-decay, the proton emission can be dealt with within the WKB barrier penetration model since the decay process can be treated in a simple quantum tunneling effect through a potential barrier. Several approaches have been used to calculate the half-lives of spherical proton emitters such as density-dependent M3Y (DDM3Y) effective interaction [3, 4], JLM interaction [4], distorted-wave Born approximation [5, 6] and unified fission model (UFM) [7]. In this work, we employ the UFM improved from the previous UFM of M. Balasubramaniam and N. Arunachalamto to study the proton emission.

2 The method

In the UFM, half-life can be obtained by $T_{\rm p} = \ln 2/(\nu_0 P)$ without introducing spectroscopic factor. Here ν_0 is the assault frequency that will be discussed in detail later. The barrier penetrability P is calculated within the action integral

$$P = \exp\left[-\frac{2}{\hbar}\int_{R_{\rm in}}^{R_{\rm out}} \sqrt{2\mu(V(r)-Q)}\ {\rm d}r\right], \qquad (1)$$

where $R_{\rm in}$ and $R_{\rm out}$ are the first and second turning points with $V(R_{\rm in}) = V(R_{\rm out}) = Q$. The potential $V(r)$ is composed of the repulsive Coulomb potential, the attractive nuclear proximity potential

Received 25 March 2009

* Supported by National Science Foundation of China (10775061, 10505016, 10575119), Fundamental Research Fund for Physics and Mathematics of Lanzhou University (LZULL200805), CAS Knowledge Innovation Project (KJCX-SYW-N02) and Major State Basic Research Developing Program of China (2007CB815004)

1) E-mail: zhanghongfei@lzu.edu.cn

and centrifugal potential for $r \geqslant R_1+R_2$, but for $r<R_1+R_2$, $V(r)$ is parameterized simply as a polynomial. Here R_0, R_1 and R_2 are the radii of parent nucleus, daughter nucleus and the emitted proton respectively, which are given by [7]:

$$R_i=(1.28A_i^{1/3}-0.76+0.8A_i^{-1/3})\ \text{fm},\quad i=0,1,2. \tag{2}$$

In a word, the potential $V(r)$ is given by:

$$V(r)=\begin{cases} a_0+a_1r+a_2r^2 & \text{for } R_0\leqslant r<R_1+R_2 \\ V_\text{p}(r)+V_\ell(r)+\dfrac{Z_1Z_2e^2}{r} & \text{for } r\geqslant R_1+R_2, \end{cases} \tag{3}$$

where Z_1 and Z_2 are the charge number of the emitted particle and daughter nucleus, respectively. The coefficient a_0, a_1, a_2 in the polynomial can be determined by the following boundary conditions:

(1) At $r=R_0=R_\text{in}$, $V(r)=Q$;

(2) At $r=R_1+R_2$, $V(r)=V(R_1+R_2)$;

(3) At $r=R_1+R_2$, $\dfrac{\text{d}V(r)}{\text{d}r}=\dfrac{\text{d}V(R_1+R_2)}{\text{d}r}$.

The third condition ensures that the potential curve is smooth, which is different from the previous UFM. Here R_in equals the radius R_0 of parent nucleus and R_out is given by:

$$R_\text{out}=\frac{Z_1Z_2e^2}{2Q}+\sqrt{\left(\frac{Z_1Z_2e^2}{2Q}\right)^2+\frac{\ell(\ell+1)\hbar^2}{2\mu Q}}\,. \tag{4}$$

The $V_\text{p}(r)$ in potential is the nuclear proximity potential that can be found in Refs. [7, 8] and we do not show it here. The proximity potential has also been introduced into the generalized liquid drop model (GLDM) [9, 10] with different formula, but it vanishes when there is no gap or neck there, which differs from what we discuss here. The centrifugal barrier $V_\ell(r)$ due to angular momentum of emitted particle (angular momentum transfer) takes the form:

$$V_\ell(r)=\frac{\ell(\ell+1)\hbar^2}{2\mu r^2}\,, \tag{5}$$

where ℓ and μ are the orbit angular momentum (without dimension) of emitted particle and the reduced mass of the two body system, respectively.

We assume that the proton which will emit vibrates nearby the surface of the parent nucleus in a harmonic oscillator potential $V(r)=-V_0+\frac{1}{2}\mu\omega^2r^2$ with classical frequency ω and reduced mass μ. By employing the virtual theorem, we obtain

$$\mu\omega^2\overline{r^2}=\left(2n_r+\ell+\frac{3}{2}\right)\hbar\omega\,, \tag{6}$$

where n_r and the ℓ are the radial quantum number (corresponding to number of nodes) and angular momentum quantum number, respectively. $\langle\psi|r^2|\psi\rangle^{1/2}$ is the root mean square (rms) radius of outermost proton distributions in quantum mechanics and that it is assumed to be equal to the rms radius R_n of the nucleus here. It is farfetched that the assault frequency is understood with a classical method that particle moves back and forth inside the nucleus due to the wave properties of particle. We take the oscillation frequency ν_0 as the assault frequency, which is related to oscillation frequency ω:

$$\nu_0=\frac{\omega}{2\pi}=\frac{\left(2n_r+\ell+\frac{3}{2}\right)\hbar}{2\pi\mu R_\text{n}^2}=\frac{\left(G+\frac{3}{2}\right)\hbar}{1.2\pi\mu R_0^2}\,. \tag{7}$$

The relationship of $R_\text{n}^2=\frac{3}{5}R_0^2$ [11] is used here. $G=2n_r+\ell$ is the principal quantum number. For proton emission we choose $G=4$ or 5 corresponding to $4\hbar\omega$ or $5\hbar\omega$ oscillator shell depending on different nuclei. The order of magnitude of ν_0 is 10^{21} s^{-1}.

3 Numerical calculations and results

Table 1 presents our calculated half-lives of different spherical proton emitters with the experimental Q values. The experimental data of ^{155}Ta and ^{159}Re are taken from Ref. [12] and Ref. [14], respectively and their Q values are calculated using the measured emitted proton energies. Other experimental data are from Ref. [1]. The results obtained with the DDM3Y and JLM models have been shown for comparison. The DDM3Y and JLM models are very successful due to the appropriate considerations in the microscopic level. A comparison has been made with the experimental logarithm of half-lives, the DDM3Y and JLM ones show that the UFM combining with the phenomenological assault frequency could provide reliable results as good as DDM3Y and JLM models. As the DDM3Y and JLM models, the half-lives of ^{177}Tl (in isomeric state) and ^{185}Bi being off by an order of magnitude are poor agreement with the experimental data, which is due to the small spectroscopic factors. Recently, the spherical proton emitter ^{155}Ta was observed whose Q value and half-life have been measured again [12]. With the proton energy $E_\text{p}=1.444\pm0.015$ MeV ($Q=1.453\pm0.015$ MeV), we obtain $T_\text{p}=9.95^{+3.62}_{-2.62}$ ms using the UFM with $\ell=5$ [13] compared with the experimental data of $T_\text{p}=2.9^{+1.5}_{-1.1}$ ms. The Q value is compatible with the half-life according to our calculation, which indicates the experimental data should be reliable. The new spherical proton emitter ^{159}Re was synthesized in the reaction ^{106}Cd (^{58}Ni, p4n) ^{159}Re [14] and its proton emission Q value along with half-life has been measured recently. The Q value is compatible with the half-life with angular momentum transfer $\ell = 5$ according to our calculation, which indicates the proton is emitted from an $h_{11/2}$ state agreeing with the conclusion in Ref. [14]. Since centrifugal potential barrier is much lower than the Coulomb potential barrier, the ratio of the $T_p(\ell)$ with nonzero ℓ to $T_p(\ell)$ with $\ell=0$ could be obtained:

Table 1. Comparisons between experimental and calculated proton emission logarithmic half-lives of spherical proton emitters. The asterisk(*) symbols in parent nuclei denote the isomeric states.

parent	ℓ	Q/MeV expt.	$\lg T_p$/s expt.	$\lg T_p$/s UFM	$\lg T_p$/ s DDM3Y[3]	$\lg T_p$/s DDM3Y[4]	$\lg T_p$/s JLM[4]
^{105}Sb	2	0.491(15)	$2.049^{+0.058}_{-0.067}$	$2.014^{+0.478}_{-0.456}$	1.97(46)	2.27(46)	1.69(45)
^{145}Tm	5	1.753(10)	$-5.409^{+0.109}_{-0.146}$	$-5.140^{+0.064}_{-0.064}$	−5.14(6)	−5.20(6)	−5.10(6)
^{147}Tm	5	1.071(3)	$0.591^{+0.125}_{-0.175}$	$1.073^{+0.040}_{-0.040}$	0.98(4)	0.98(4)	1.07(4)
^{147}Tm*	2	1.139(5)	$-3.444^{+0.046}_{-0.051}$	$-3.086^{+0.060}_{-0.060}$	−3.39(5)	−3.26(6)	−3.27(6)
^{150}Lu	5	1.283(4)	$-1.180^{+0.055}_{-0.064}$	$-0.852^{+0.042}_{-0.042}$	−0.58(4)	−0.59(4)	−0.49(4)
^{150}Lu*	2	1.317(15)	$-4.523^{+0.620}_{-0.301}$	$-4.421^{+0.150}_{-0.147}$	−4.38(15)	−4.24(15)	−4.24(15)
^{151}Lu	5	1.255(3)	$-0.896^{+0.011}_{-0.012}$	$-0.568^{+0.032}_{-0.032}$	−0.67(3)	−0.65(3)	−0.55(3)
^{151}Lu*	2	1.332(10)	$-4.796^{+0.026}_{-0.027}$	$-4.577^{+0.098}_{-0.097}$	−4.88(9)	−4.72(10)	−4.73(10)
^{155}Ta	5	1.453(15)	$-2.538^{+0.181}_{-0.207}$	$-2.002^{+0.135}_{-0.133}$	−4.65(6)	−4.67(6)	−4.57(6)
^{156}Ta	2	1.028(5)	$-0.620^{+0.082}_{-0.101}$	$-0.339^{+0.074}_{-0.074}$	−0.38(7)	−0.22(74)	−0.23(7)
^{156}Ta*	5	1.130(8)	$0.949^{+0.100}_{-0.129}$	$1.454^{+0.104}_{-0.103}$	1.66(10)	1.66(10)	1.76(10)
^{157}Ta	0	0.947(7)	$-0.523^{+0.135}_{-0.198}$	$-0.015^{+0.117}_{-0.116}$	-0.43(11)	−0.21(11)	−0.23(11)
^{159}Re	5	1.816(20)	$-4.678^{+0.076}_{-0.092}$	$-4.330^{+0.133}_{-0.131}$	–	–	–
^{160}Re	2	1.284(6)	$-3.046^{+0.075}_{-0.056}$	$-2.957^{+0.065}_{-0.065}$	−3.00(6)	−2.86(6)	−2.87(6)
^{161}Re	0	1.214(6)	$-3.432^{+0.045}_{-0.049}$	$-3.059^{+0.071}_{-0.071}$	−3.46(7)	−3.28(7)	−3.29(7)
^{161}Re*	5	1.338(7)	$-0.488^{+0.056}_{-0.065}$	$-0.421^{+0.073}_{-0.072}$	−0.60(7)	−0.57(7)	−0.49(7)
^{164}Ir	5	1.844(9)	$-3.959^{+0.190}_{-0.139}$	$-4.114^{+0.060}_{-0.059}$	−3.92(5)	−3.95(5)	−3.86(5)
^{165}Ir*	5	1.733(7)	$-3.469^{+0.082}_{-0.100}$	$-3.359^{+0.051}_{-0.050}$	−3.51(5)	−3.52(5)	−3.44(5)
^{166}Ir	2	1.168(8)	$-0.824^{+0.166}_{-0.273}$	$-1.008^{+0.103}_{-0.102}$	−1.11(10)	v0.96(10)	−0.96(10)
^{166}Ir*	5	1.340(8)	$-0.076^{+0.125}_{-0.176}$	$0.064^{+0.085}_{-0.084}$	0.21(8)	0.22(8)	0.30(8)
^{167}Ir	0	1.086(6)	$-0.959^{+0.024}_{-0.025}$	$-0.774^{+0.086}_{-0.086}$	−1.27(8)	−1.05(8)	−1.07(8)
^{167}Ir*	5	1.261(7)	$0.875^{+0.098}_{-0.127}$	$0.928^{+0.082}_{-0.081}$	0.69(8)	0.74(8)	0.81(8)
^{171}Au	0	1.469(17)	$-4.770^{+0.185}_{-0.151}$	$-4.588^{+0.160}_{-0.157}$	−5.02(15)	−4.84(15)	−4.86(15)
^{171}Au*	5	1.718(6)	$-2.654^{+0.054}_{-0.060}$	$-2.837^{+0.045}_{-0.045}$	−3.03(4)	−3.03(4)	−2.96(4)
^{177}Tl	0	1.180(20)	$-1.174^{+0.191}_{-0.349}$	$-0.800^{+0.270}_{-0.263}$	−1.36(25)	−1.17(25)	−1.20(25)
^{177}Tl*	5	1.986(10)	$-3.347^{+0.095}_{-0.122}$	$-4.271^{+0.062}_{-0.062}$	−4.49(6)	−4.52(5)	−4.46(5)
^{185}Bi	0	1.624(16)	$-4.229^{+0.068}_{-0.081}$	$-4.949^{+0.136}_{-0.134}$	−5.44(13)	−5.33(13)	−5.36(13)

$$\frac{T_p(\ell)}{T_p(0)} \approx \frac{\exp\left\{-2\int_{R_{in}}^{R_{out}}\sqrt{\frac{2\mu}{\hbar^2}\left[V_p+\frac{(Z-1)e^2}{r}-Q\right]}\mathrm{d}r\right\}}{\exp\left\{-2\int_{R_{in}}^{R_{out}}\sqrt{\frac{2\mu}{\hbar^2}\left[V_p+\frac{(Z-1)e^2}{r}+\frac{\ell(\ell+1)\hbar^2}{2\mu r^2}-Q\right]}\mathrm{d}r\right\}} \approx \exp\left[\frac{2\ell(\ell+1)}{\sqrt{\frac{2\mu}{\hbar^2}\frac{(Z-1)e^2}{R_{in}}}R_{in}}\right] \approx \exp\left[c_0\frac{\ell(\ell+1)}{\sqrt{(A-1)(Z-1)A^{-2/3}}}\right]. \quad (8)$$

where A and Z are the mass and charge numbers of the parent nucleus and the approximate relationship $R_{in}=R_0\approx r_0A^{1/3}$ fm has been used here. This formula can be further written in the following form:

$$\lg T_p(\ell)=\lg T_p(0)+c\frac{\ell(\ell+1)}{\sqrt{(A-1)(Z-1)A^{-2/3}}}. \quad (9)$$

The half-life T_p is measured in second. The c is a model-dependent parameter with c = 2.8 for the UFM. The relationships between $\lg T_p(\ell)$ and $\ell(\ell+1)$ from the UFM and the formula (9) are presented in Fig. 1 taking Ir isotopes as examples. Good agreement is found between the formula (9) and the results of UFM. The great influences of the angular momenta

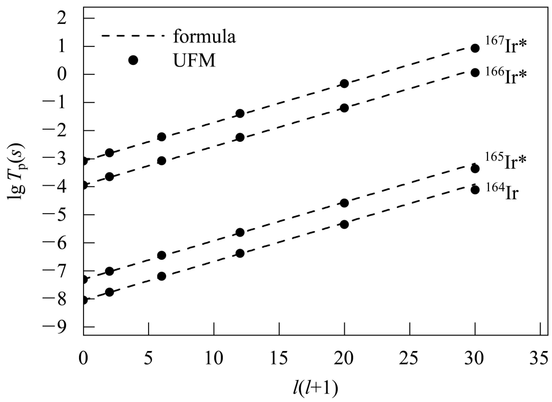

Fig. 1. Proton emission half-lives of Ir isotopes as a function of $\ell(\ell+1)$. The asterisk(*) symbol in parent nucleus denotes the isomeric state. The calculations are performed with the UFM and the formula (9).

transfers ℓ on the half-lives are visible. On account of smaller reduced mass μ compared with that in α-decay system, the centrifugal barrier for proton emission is much more important than that for α-decay. The half-life can be changed by 3–4 orders of magnitude when the angular momentum transfer is $\ell = 5$ instead of $\ell = 0$. The half-life of proton emission is quite sensitive to the angular momentum transfer ℓ, which in turn helps to determine the ℓ value by the UFM if half-life T_p and Q values are given. On the other hand, so many proton emitters can be observed in experiments due to the centrifugal barriers prolonging the lifetimes of these nuclei to a large extent.

4 Summary

In summary, the half-lives of proton emission for spherical proton emitters have been investigated in the framework of the UFM with the phenomenological assault frequency. No adjustable parameter has been involved in the calculations. Good agreement is found compared with the experimental data and other theoretical results, which indicates the UFM with the phenomenological assault frequency works well for the study of proton emission. As other theoretical results, the UFM can not provide a good explanation for proton emission half-lives of ^{177}Tl (in isomeric state) and ^{185}Bi because of their small spectroscopic factors. The effect of angular momentum transfer on half-life of proton emission has been discussed, and a formula can be employed to describe this relationship successfully.

References

1 Sonzogni A A. Nuclear Data Sheets, 2002, **95**: 1
2 Karny M et al. Phys. Lett. B, 2008, **664**: 52
3 Basu D N, chowdhury P R, Samanta C. Phys. Rev. C, 2005, **72**: 051601(R)
4 Bhattacharya M, Gangopadhyay G. Phys. Lett. B, 2007, **651**: 263
5 Aberg S, Semmes P B, Nazarewicz W. Phys. Rev. C, 1997, **56**: 1762
6 JIANG J G, REN Z Z. Chin. Phys. Lett., 2006, **23**: 812
7 Balasubramaniam M, Arunachalam N. Phys. Rev. C, 2005, **71**: 014603
8 Blocki J et al. Ann. Phys.(NY), 1977, **105**: 427
9 ZHANG H F, LI J Q, ZUO W, ZHOU X H, GAN Z G. Commun. Theor. Phys., 2007, **48**: 545
10 DONG J M, ZHANG H F, ZUO W, LI J Q. Chin. Phys. Lett., 2008, **25**: 4230
11 Myers W D, Swiatecki W J. Phys. Rev. C, 2000, **62**: 044610
12 Page R D et al. Phys. Rev. C, 2007, **75**: 061302(R)
13 Delion D S, Liotta R J, Wyss R. Phys. Rev. Lett., 2006, **96**: 072501
14 Joss D T et al. Phys. Lett. B, 2006, **641**: 34